Development 138, 4609-4619 (2011) doi:10.1242/dev.067165
© 2011. Published by The Company of Biologists Ltd

Hesr1 and Hesr3 are essential to generate undifferentiated quiescent satellite cells and to maintain satellite cell numbers

So-ichiro Fukada[1,*], Masahiko Yamaguchi[1], Hiroki Kokubo[2], Ryo Ogawa[1], Akiyoshi Uezumi[3], Tomohiro Yoneda[1], Miroslav M. Matev[1], Norio Motohashi[4], Takahito Ito[1], Anna Zolkiewska[5], Randy L. Johnson[6], Yumiko Saga[2], Yuko Miyagoe-Suzuki[4], Kazutake Tsujikawa[1], Shin'ichi Takeda[4] and Hiroshi Yamamoto[1]

SUMMARY

Satellite cells, which are skeletal muscle stem cells, divide to provide new myonuclei to growing muscle fibers during postnatal development, and then are maintained in an undifferentiated quiescent state in adult skeletal muscle. This state is considered to be essential for the maintenance of satellite cells, but their molecular regulation is unknown. We show that *Hesr1* (*Hey1*) and *Hesr3* (*Heyl*) (which are known Notch target genes) are expressed simultaneously in skeletal muscle only in satellite cells. In *Hesr1* and *Hesr3* single-knockout mice, no obvious abnormalities of satellite cells or muscle regenerative potentials are observed. However, the generation of undifferentiated quiescent satellite cells is impaired during postnatal development in *Hesr1/3* double-knockout mice. As a result, myogenic (MyoD and myogenin) and proliferative (Ki67) proteins are expressed in adult satellite cells. Consistent with the in vivo results, *Hesr1/3*-null myoblasts generate very few $Pax7^+$ $MyoD^-$ undifferentiated cells in vitro. Furthermore, the satellite cell number gradually decreases in *Hesr1/3* double-knockout mice even after it has stabilized in control mice, and an age-dependent regeneration defect is observed. In vivo results suggest that premature differentiation, but not cell death, is the reason for the reduced number of satellite cells in *Hesr1/3* double-knockout mice. These results indicate that Hesr1 and Hesr3 are essential for the generation of adult satellite cells and for the maintenance of skeletal muscle homeostasis.

KEY WORDS: Satellite cells, Undifferentiated quiescent state, Hesr1 (Hey1), Hesr3 (Heyl), Mouse

INTRODUCTION

Satellite cells, which are muscle-specific stem cells, are anatomically identified as mononuclear cells that reside external to the myofiber plasma membrane and beneath the basal lamina (Mauro, 1961). During postnatal development, satellite cells divide to provide new myonuclei to growing muscle fibers (Moss and Leblond, 1971), and then change to an undifferentiated quiescent state in adult skeletal muscle (Schultz et al., 1978). This state is considered essential for sustaining the satellite cell compartment.

Skeletal muscle regeneration also depends on satellite cells. When muscles are damaged, satellite cells exit from quiescence and start to proliferate. Proliferating satellite cells, called myoblasts, then differentiate, fuse with each other or with injured myofibers, and eventually regenerate mature myofibers (Charge and Rudnicki, 2004). The activation, proliferation and differentiation of satellite cells are mainly controlled by the myogenic regulatory factors, a group of skeletal muscle-specific basic helix-loop-helix (bHLH) transcription factors comprising MyoD (also known as Myod1), Myf5, myogenin and Mrf4 (also known as Myf6). Myogenin and Mrf4 are crucial for the late stages of myogenic differentiation (Sabourin and Rudnicki, 2000). The *Myf5* locus is active in most quiescent satellite cells (Beauchamp et al., 2000). By contrast, quiescent satellite cells do not express MyoD, but start to express it when they are activated and start to proliferate (Zammit et al., 2004). During regeneration, MyoD is essential for the proliferation of satellite cell-derived myoblasts (Megeney et al., 1996). A recent study showed that entry of quiescent myogenic cells into the S phase of the cell cycle requires MyoD expression (Zhang et al., 2010). Therefore, the molecular mechanism that upregulates MyoD expression is key to satellite cell activation, whereas MyoD suppression in quiescent satellite cells seems to be essential for maintaining the satellite cell pool in an undifferentiated quiescent state.

The Notch signaling pathway is an evolutionarily conserved intercellular signaling system that has multiple essential roles in cell fate decisions and in patterning events (Lai, 2004). When Notch is activated, the intracellular domain of Notch is cleaved by γ-secretase and translocates to the nucleus where it activates the transcription of target genes through interaction with Rbpj (also known as Cbf1). It is well known that the Hes (Hairy and enhancer of split) and Hesr (Hes-related, also known as Hey/Herp/Hrt/Gridlock/Chf) families of bHLH transcriptional repressor genes are the primary target of Notch signaling and play important roles in nerve, heart and vascular development, among others (Fischer and Gessler, 2007). In the case of myogenic cells, it has been reported that the activation of Notch signaling by delta-like 1 (Dll1), one of the Notch ligands, inhibits MyoD expression in C2C12 cells (a myogenic cell line) (Kuroda et al., 1999) and in

[1]Department of Immunology, Graduate School of Pharmaceutical Sciences, Osaka University, 1-6 Yamada-oka, Suita, Osaka 565-0871, Japan. [2]Division of Mammalian Development, National Institute of Genetics, Mishima, Shizuoka 411-8540, Japan. [3]Division for Therapies Against Intractable Diseases, Institute for Comprehensive Medical Science, Fujita Health University, 1-98 Dengakugakubo, Kutsukake, Toyoake, Aichi 470-1192, Japan. [4]Department of Molecular Therapy, National Institute of Neuroscience, National Center of Neurology and Psychiatry, 4-1-1 Ogawa-higashi, Kodaira, Tokyo 187-8502, Japan. [5]Department of Biochemistry, Kansas State University, Manhattan, KS 66506, USA. [6]Department of Biochemistry and Molecular Biology, University of Texas, M.D. Anderson Cancer Center, 1515 Holcomb Blvd, Houston TX 77030, USA.

*Author for correspondence (fukada@phs.osaka-u.ac.jp)

Accepted 30 August 2011

avian myotomal cells (Hirsinger et al., 2001). Furthermore, Kuang et al. reported that, in vitro, the number of Pax7^{+} MyoD^{-} undifferentiated satellite cells was significantly decreased when proliferating satellite cells were treated with DAPT, an inhibitor of γ-secretase (Kuang et al., 2007). These results indicate the important roles of Notch signaling in myogenic cells, but the roles of the transcriptional targets of Notch signaling in myogenic cells, including satellite cells, remain largely unknown.

In this study, we show that Hesr1 and Hesr3 are important regulators that are responsible for the generation of undifferentiated quiescent satellite cells and for the maintenance of satellite cell numbers. Our findings have implications for the roles of Hesr family genes in the maintenance of tissue homeostasis and facilitate investigation of the molecular regulation of satellite cells.

MATERIALS AND METHODS

Mice

Hesr1$^{-/-}$ mice were described previously (Kokubo et al., 2005b). *Hesr3*$^{-/-}$ mice were generated by H.K. (unpublished). To generate *Hesr1*$^{-/-}$ *Hesr3*$^{-/-}$ mice, *Hesr1*$^{+/-}$ *Hesr3*$^{-/-}$ and *Hesr1*$^{+/-}$ *Hesr3*$^{-/-}$ mice were crossed. All procedures for experimental animals were approved by the Experimental Animal Care and Use Committee at Osaka University.

Muscle injury

Muscle injury was induced by injecting 2.5 μl 10 μM (in saline) cardiotoxin (Wako Pure Chemical Industries, Tokyo, Japan) per gram mouse body weight into the tibialis anterior (TA) muscle.

RT-PCR

Total RNA was extracted from sorted or cultured cells using the RNeasy Mini Kit according to the manufacturer's instructions (Qiagen, Hilden, Germany) and then reverse-transcribed into cDNA using TaqMan reverse transcription reagents (Roche Diagnostics, Mannheim, Germany). PCR was performed with the cDNA using the primers listed in Table S1 in the supplementary material.

Real-time PCR was performed using SYBR Premix Ex Taq (Takara, Kyoto, Japan) in a final reaction volume of 10 μl. Specific forward and reverse primers for optimal amplification in real-time PCR of reverse-transcribed cDNAs were used (see Table S1 in the supplementary material). Real-time PCR and data analyses were performed on a LightCycler Quick System 350S using LightCycler Software (Roche Diagnostics). Samples were amplified and the relative gene expression levels were calculated using standard curves generated by serial dilutions of the cDNA.

Histological analyses

TA muscles were isolated and frozen in liquid nitrogen-cooled isopentane (Wako Pure Chemical Industries). Transverse cryosections (10 μm) were stained with Hematoxylin and Eosin (H&E), Oil Red O (Sigma-Aldrich, St Louis, MO, USA), or Sirius Red (Sigma-Aldrich).

Immunocytochemistry and immunohistochemistry

For immunohistochemical examinations, transverse cryosections (6 μm) were fixed with 4% PFA for 10 minutes. For eMyHC staining, the sections were fixed with cooled acetone for 10 minutes at –20°C. After blocking with 5% skimmed milk, sections were stained with primary antibodies. Antibodies used are listed in Table 1.

For Pax7 and eMyHC staining, an M.O.M. Kit (Vector Laboratories, Burlingame, CA, USA) was used to block endogenous mouse IgG. After the first staining at 4°C overnight, sections were incubated with secondary antibodies conjugated with Alexa Fluor 488, 568 or 647 (Molecular Probes, Eugene, OR, USA). For EdU detection, the Click chemical reaction was performed after primary and secondary staining according to the manufacturer's instructions using a Click-iT EdU Imaging Kit (Invitrogen, Carlsbad, CA, USA). Coverslips were mounted using Vectashield (Vector Laboratories).

Cultured cells were fixed with 4% PFA for 10 minutes and then permeabilized with 0.1% Triton X-100 in PBS for 20 minutes. After blocking with 5% skimmed milk, the cells were stained as described above. The signals were recorded photographically using a confocal laser-scanning microscope system (TCS-SP5, Leica, Heerbrugg, Switzerland) or a fluorescence microscope (BX51, Olympus, Tokyo, Japan) equipped with a DP70 CCD camera (Olympus).

Preparation and FACS analyses of skeletal muscle-derived mononuclear cells

Mononuclear cells from uninjured limb muscles were prepared using 0.2% collagenase type II (Worthington Biochemical, Lakewood, NJ, USA) as previously described (Uezumi et al., 2006).

Table 1. Antibodies

Antibody	Clone	Ig type	Conjugate	Supplier	Application and dilution
Primary antibodies					
CD31	390	Rat IgG2a, κ	FITC	BD Pharmingen	FACS, 1:400
CD45	30-F11	Rat IgG2b, κ	FITC	BD Pharmingen	FACS, 1:800
Sca1	D7	Rat IgG2a, κ	PE	BD Pharmingen	FACS, 1:400
Satellite cells	SM/C-2.6	Rat IgG2a	Biotin	Fukada et al., 2004	FACS, 1:200
laminin α2	4H8-2	Rat IgG1	–	Alexis	IHC, 1:200
Pax7	PAX7	Mouse IgG1, κ	–	DSHB	IHC, 1:2 (supernatant)
M-cadherin	Polyclonal	Rabbit IgG	–	S.T.	IHC, 1:1000
calcitonin receptor	Polyclonal	Rabbit IgG	–	AbD Serotec	IHC, 1:100
MyoD	Polyclonal	Rabbit IgG	–	Santa Cruz	IHC, 1:200
MyoD	5.8A	Mouse IgG1, κ	–	BD Pharmingen	IHC, 1:200
myogenin	F5D	Mouse IgG1, κ	–	DSHB	IHC, 1:30
Ki67	Polyclonal	Rabbit IgG	–	Ylem	IHC, 1:2
Ki67	Polyclonal	Rabbit IgG	–	Abcam	IHC, 1:100
Sarcomeric α-actinin	EA-53	Mouse IgG1	–	Sigma	ICC, 1:100
eMyHC	F1.652	Mouse IgG	–	DSHB	IHC, 1:2
Hesr3	Polyclonal	Rabbit IgG	–	Fukada et al., 2007	IHC, 1:200
Secondary antibodies					
Rat IgG	–	Goat	Alexa Fluor 568	Molecular Probes	IHC, 1:1000
Mouse IgG	–	Goat	Alexa Fluor 568	Molecular Probes	IHC, 1:1000; ICC, 1:1000
Mouse IgG	–	Donkey	Alexa Fluor 488	Molecular Probes	IHC, 1:1000
Rabbit IgG	–	Goat	Alexa Fluor 488	Molecular Probes	IHC, 1:1000
Rat IgG	–	Chicken	Alexa Fluor 647	Molecular Probes	IHC, 1:1000

DSHB, Developmental Studies Hybridoma Bank; FACS, fluorescence-activated cell sorting; IHC, immunohistochemistry; ICC, immunocytochemistry.

Mononuclear cells derived from skeletal muscle were stained with FITC-conjugated anti-CD31 (Pecam1 – Mouse Genome Informatics), anti-CD45 (Ptprc – Mouse Genome Informatics), phycoerythrin-conjugated anti-Sca1 (Ly6a – Mouse Genome Informatics) and biotinylated SM/C-2.6 (Fukada et al., 2004) antibodies. Cells were then incubated with 1:400 streptavidin-allophycocyanin (APC) (BD Biosciences, San Diego, CA, USA) on ice for 30 minutes, and resuspended in PBS containing 2% FCS and 2 μg/ml propidium iodide (PI). Cell sorting was performed using a FACS Aria II flow cytometer (BD Immunocytometry Systems, Mountain View, CA, USA). Debris and dead cells were excluded by forward scatter, side scatter and PI gating. Data were collected using FACSDiva software (BD Biosciences). Myogenic cells from the regenerating muscle were also highly enriched in the SM/C-2.6$^+$ CD31$^-$ CD45$^-$ Sca1$^-$ cell fraction (Segawa et al., 2008).

Satellite cell culture

Freshly isolated satellite cells were cultured in a growth medium (GM) of high-glucose Dulbecco's modified Eagle's medium (DMEM-HG; Sigma-Aldrich) containing 20% FCS (Trace Biosciences, N.S.W., Australia), 2.5 ng/ml bFGF (FGF2) (PeproTech, London, UK), and penicillin (100 U/ml)-streptomycin (100 μg/ml) (Gibco BRL, Gaithersburg, MD, USA) on culture dishes coated with Matrigel (BD Biosciences). Differentiation was induced in differentiation medium (DM) containing DMEM-HG, 5% horse serum and penicillin-streptomycin for 3-4 days.

Co-culture with CHO-Dll1

Satellite cells were isolated from C57BL/6 mice and 1×10^5 cells were plated in six-well plates. Three days later, CHO cells stably transfected with mouse Dll1 or empty vector (Dyczynska et al., 2007) were added (5×10^5 cells/well) and incubated in GM without G418. After 24 hours, total RNA was extracted from the cultured cells.

Detection of apoptotic cells

Freshly isolated satellite cells were cultured on eight-well Lab-Tek chamber slides (Nunc, Rochester, NY, USA) in GM. After culturing for 24 hours, apoptotic cells were detected by Rhodamine fluorescence using the ApopTag Red In Situ Apoptosis Detection Kit (Chemicon, Temecula, CA, USA).

In vitro cell proliferation assay

Isolated satellite cells were cultured on eight-well Lab-Tek chamber slides in GM for 2-3 days, and then EdU (final concentration 10 μm; Invitrogen) was added. After additional culture for 12 hours, cells were fixed and stained following the protocol supplied by the manufacturer (Invitrogen). Three to six random fields per sample were counted.

Clonal analysis

Single cell sorting was performed using the FACS Aria II. Sorted cells were grown in GM on Matrigel-coated 96-well dishes. During 7 days of culture, cell number and frequency of colony formation from a single satellite cell were quantified.

In vivo EdU-uptake assay

EdU was dissolved in PBS at 0.5 mg/ml and injected intraperitoneally at 0.1 mg per 20 g body weight at the time points indicated.

Measurement of myofiber area

ImageJ software was used to measure myofiber size and eMyHC-positive, Oil Red O-positive and Sirius Red-positive areas per section. To calculate the TA myofiber area, 80-145 myofibers per mouse were examined. Graphs representing myofiber areas were generated and analyzed by ANOVA.

Statistics

Values are expressed as mean ± s.d. Statistical significance was assessed by Student's *t*-test. In comparisons of more than two groups, non-repeated measures analysis of variance (ANOVA) followed by the Bonferroni test (versus control) or the Student-Newman-Keuls (SNK) test (multiple comparisons) was used. $P<0.05$ or $P<0.01$ was considered statistically significant.

RESULTS

Expression of Hesr family genes in muscle satellite cells

The Hesr family comprises three members: *Hesr1* (*Hey1*/*Hrt1*/*Herp2*), *Hesr2* (*Hey2*/*Hrt2*/*Herp1*) and *Hesr3* (*Heyl*/*Hrt3*/*Herp3*). In a previous study (Fukada et al., 2007), we identified the most highly expressed genes in adult quiescent satellite cells by comparing them with activated/proliferating satellite cells and non-myogenic cells. *Hesr3*, a known Notch effector gene, is one of these genes, being highly expressed in quiescent satellite cells but not in myofibers. Hesr3 protein expression was also confirmed in quiescent satellite cells, but not in cultured activated/proliferating satellite cells (Fig. 1A, see Fig. S1A in the supplementary material). As shown in Fig. 1B, *Hesr1* is also expressed in quiescent satellite cells. However, in contrast to *Hesr3*, a weak *Hesr1* signal was detected in activated/proliferating satellite cells cultured for 3 days (myoblasts). *Hesr2* was expressed in neither quiescent satellite cells nor myoblasts.

To reveal the expression of *Hesr1* and *Hesr3* in adult skeletal muscle, mononuclear cells derived from uninjured skeletal muscle were separated into four fractions using CD31 as an endothelial marker, SM/C-2.6 as a satellite cell marker (Fukada et al., 2004), and Sca1 as a fibro/adipogenic cell or mesenchymal progenitor marker (Joe et al., 2010; Uezumi et al., 2010). The expression of *Pax7* and *Myf5* in the isolated CD31$^-$ Sca1$^-$ SM/C-2.6$^+$ cells confirmed the purity of the satellite cell population (Fig. 1C). Consistent with our previous study, *Hesr3* was expressed exclusively in muscle satellite cells in normal skeletal muscle, whereas both satellite cells and endothelial cells expressed *Hesr1*. *Hesr3* was identified as an adult quiescent satellite cell gene. However, neonatal proliferating satellite cells expressed *Hesr1* and *Hesr3* (see Fig. S1B,C in the supplementary material). In vivo proliferating satellite cells showed similar results to cultured myoblasts (see Fig. S1B,C in the supplementary material). Therefore, in some aspects, neonatal satellite cells are different from regenerating satellite cells, as previously described (Pallafacchina et al., 2010).

Hesr1 or *Hesr3* single-knockout mice show no obvious skeletal muscle phenotype

To determine the function of Hesr genes in skeletal muscle and satellite cells, we first investigated *Hesr1* and *Hesr3* single-knockout mice. It was previously reported that *Hesr1* (1KO) and *Hesr3* (3KO) knockout mice show no abnormalities in fertility or life expectancy, or any major developmental defect (Fischer et al., 2004; Fischer et al., 2007; Kokubo et al., 2005a). Consistent with these studies, skeletal muscle weight as a proportion of total body weight was similar in 1KO and 3KO mice to that of littermate wild-type (WT) mice (Fig. 1D). No obvious defects in satellite cell number or regeneration ability were observed in either single-knockout mouse (Fig. 1E,F). Because restricted co-expression of *Hesr1* and *Hesr3* was observed in muscle satellite cells, we generated double-knockout (dKO) mice to examine the roles of *Hesr1*/*3* in satellite cells.

Hesr1/*3* double-knockout mice exhibit decreased body and skeletal muscle weights

Fischer et al. reported that the survival of *Hesr1*/*3* dKO mice depends on the genetic background (Fischer et al., 2007). In the F2 and F9 backcross generation into C57BL/6 mice, ~90% and less than 5%, respectively, of the dKO mice survived the first 3 weeks

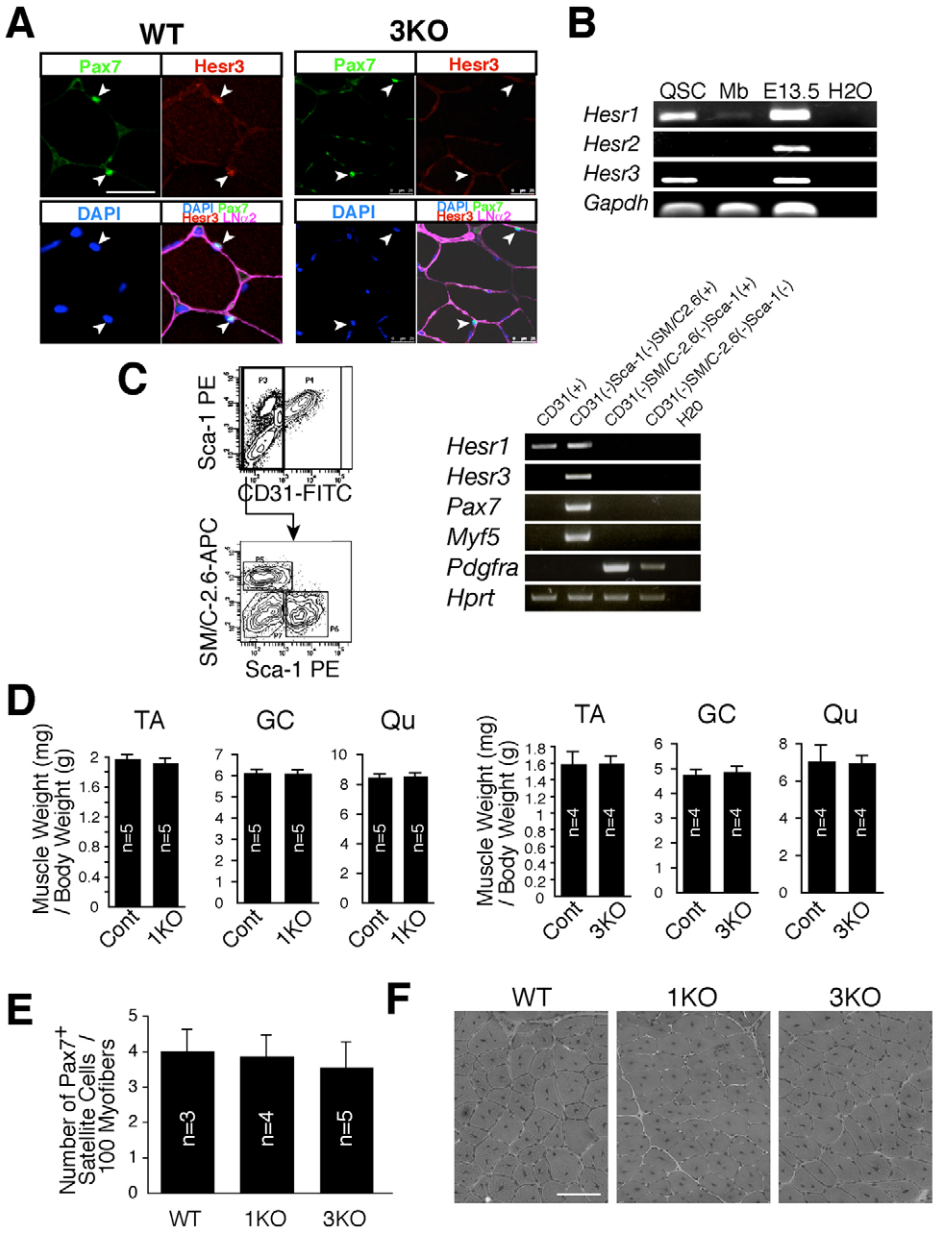

Fig. 1. Expression of Hesr family genes and the *Hesr1*-null and *Hesr3*-null skeletal muscle phenotypes. (**A**) Transverse sections of tibialis anterior muscle from wild-type (WT) and *Hesr3*-null (3KO) mice (a negative control for anti-Hesr3 antibody) were stained with antibodies to laminin α2 (violet), Pax7 (green) and Hesr3 (red) and with DAPI (blue). Arrowheads indicate Pax7-expressing cells lying beneath the basal lamina. (**B**) RT-PCR of Hesr family genes in quiescent satellite cells (QSC) and myoblasts [Mb; cultured for 3 days in growth medium (GM)]. A whole E13.5 embryo and water were used as positive and negative controls, respectively. (**C**) RT-PCR of *Hesr1* and *Hesr3* in mononuclear cells derived from 10-week-old uninjured skeletal muscle. FACS profiles show each cell population used in RT-PCR. (**D**) Tibialis anterior (TA), gastrocnemius (GC) and quadriceps (Qu) muscle weight (mg) per gram body weight of 3-month-old male *Hesr1*-null (1KO), 9-month-old male 3KO and control littermate (cont) mice. The *y*-axis shows the mean with s.d. (**E**) The number of Pax7$^+$ satellite cells in 10-week-old female uninjured TA muscle of WT, 1KO and 3KO mice. The *y*-axis shows the mean number of satellite cells per 100 cross-sectional myofibers with s.d. (**F**) A TA muscle of each 8-week-old mouse was injected with cardiotoxin and the muscles were fixed 2 weeks after the injection. The number of mice used in each study is indicated. Scale bars: 25 μm in A; 100 μm in F.

after birth. To obtain an adequate number of adult dKO mice for our analyses, we crossed F7 *Hesr*$^{+/-}$ *Hesr3*$^{-/-}$ mice and obtained ~40% dKO mice in the expected Mendelian ratio at 4 weeks of age. As littermate control mice, we used 3KO mice because they showed no apparent phenotype.

In contrast to the 1KO and 3KO results, compared with littermate control mice the dKO mice showed a slight decrease in body size and a significant decrease in body weight regardless of gender (see Fig. S2A in the supplementary material). Furthermore, 56- to 90-day-old dKO and 3KO mice exhibited a significant difference in muscle weight (see Fig. S2B in the supplementary material). The loss of muscle weight did not simply reflect the decreased body weight because there was also a significant difference in muscle weight as a proportion of body weight between dKO and littermate 3KO mice (Fig. 2A).

To assess the cause of muscle weight loss in dKO mice, the number and size of myofibers were quantified. As shown in Fig. 2B,C, compared with 3KO mice, a decrease in both myofiber number and size was observed in dKO mice. Because satellite cells contribute physiologically to muscle growth, these results imply that there are defects in the dKO satellite cells.

Decreased number of satellite cells in dKO mice

To examine the effects of the *Hesr1/3* deficiency on satellite cells, transverse sections of 8-week-old male mouse skeletal muscles were stained with three different satellite cell-specific antibodies: anti-Pax7, anti-M-cadherin (cadherin 15) and anti-calcitonin receptor (Fukada et al., 2007). As shown in Fig. 2D,E, there were significantly fewer satellite cells in dKO than in 3KO muscles.

We also analyzed the percentage of muscle satellite cells in adult mice by flow cytometry. Consistent with the immunohistochemical results, a substantial decrease in the satellite cell fraction was observed in dKO mice (Fig. 2F,G, see Fig. S3A in the supplementary material). Intriguingly, dKO satellite cells were slightly larger than 3KO satellite cells (Fig.

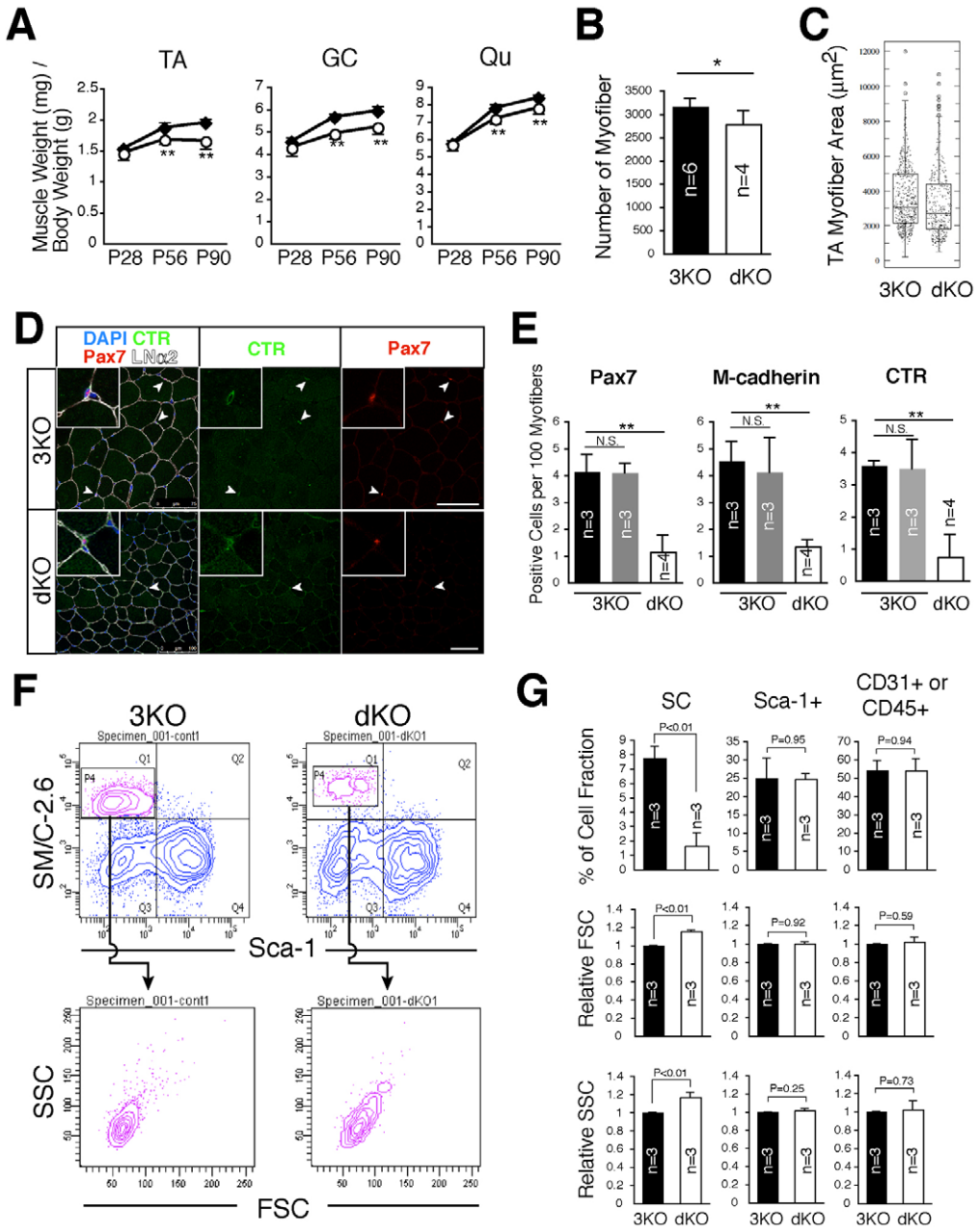

Fig. 2. Decrease in muscle weight and satellite cell number in *Hesr1/3* double-knockout (dKO) mice. (**A**) TA, GC and Qu muscle weight (mg) per gram body weight of 28-, 56- and 90-day-old male 3KO (black diamonds) and dKO (white circles) mice. The *y*-axis shows the mean with s.d. (**B**) The mean number of myofibers in uninjured TA muscle of 8-week-old male 3KO and dKO mice. The y-axis shows the mean number of myofibers per section with s.d. (**C**) The area of myofibers in B. (**D**) Transverse sections were stained for laminin α2 (white), Pax7 (red), calcitonin receptor (CTR, green) and with DAPI (blue). Arrowheads indicate Pax7-expressing cells lying beneath the basal lamina. Scale bar: 75 μm. (**E**) Satellite cell marker-positive cells in uninjured TA muscle of 8-week-old male dKO mice and 3KO littermates (black bar, *Hesr1*$^{+/+}$*Hesr3*$^{-/-}$; gray bar, *Hesr1*$^{+/-}$*Hesr3*$^{-/-}$). The *y*-axis shows the mean number of satellite cells per 100 cross-sectional myofibers with s.d. (**F**) FACS profiles of mononuclear cells derived from 13-week-old male 3KO or dKO muscles. The upper profiles were gated for CD31$^-$ CD45$^-$ fractions. The lower profiles show the cell size (FSC) and cell granularity (SSC) of satellite cell fractions (SM/C-2.6$^+$ CD31$^-$ CD45$^-$ Sca1$^-$). (**G**) The mean frequency, relative FSC and relative SSC of derived cell populations: satellite cells, CD31$^-$ CD45$^-$ Sca1$^+$; and endothelial cells or hematopoietic cells, CD31$^+$ or CD45$^+$. Thirteen- to 15-week-old mice were used. The number of mice used in each study is shown. *, *P*<0.05; **, *P*<0.01. N.S., non-significant difference.

2F,G, see Fig. S3B in the supplementary material). The frequency and cell size of the non-satellite cell population, including endothelial, hematopoietic and Sca1$^+$ CD31$^-$ CD45$^-$ cells, were not affected by the absence of both *Hesr1* and *Hesr3* (Fig. 2G). Upon activation, the organelles and volume of cytoplasm in satellite cells increase and the cells become mitotically active as they transit from the G0 to G1 cell cycle phase (Kadi et al., 2005; Fukada et al., 2007). These results suggest that the satellite cells in dKO mice were not in a quiescent state, but in a more differentiated and/or activated state.

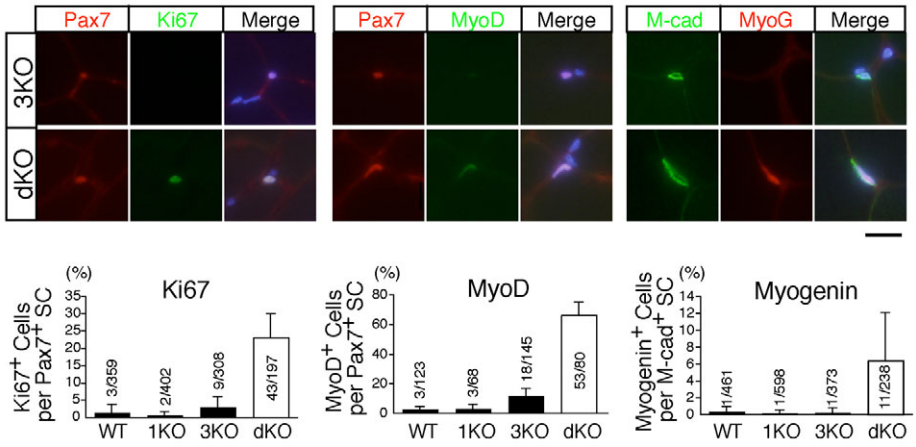

Fig. 3. Myogenic and proliferative marker expression in adult dKO satellite cells. Uninjured TA muscles of 10-week-old female dKO and 3KO mice were stained with Ki67 (green), MyoD (green) and myogenin (red) antibodies. Pax7 (red) and M-cadherin (green) antibodies were used to detect satellite cells. Scale bar: 20 μm. The graphs beneath indicate the frequency of each marker-positive cell in WT, 1KO, 3KO and dKO mice. The *y*-axis shows the mean value with s.d. (n=3-5). The number of marker-positive satellite cells among total counted satellite cells is indicated in each bar.

Increased expression of differentiation/proliferation markers in dKO satellite cells

To elucidate the expression of proliferation and myogenic differentiation markers in dKO satellite cells, transverse sections of 10-week-old female mouse tibialis anterior (TA) muscles were stained with anti-Ki67, anti-MyoD and anti-myogenin antibodies. As shown in Fig. 3, ~20% of Pax7$^+$ cells expressed Ki67, a proliferative marker that is not expressed in G0 cells. Intriguingly, in uninjured dKO skeletal muscle, ~70% of Pax7$^+$ satellite cells expressed MyoD and ~6% of M-cadherin$^+$ satellite cells expressed myogenin. In contrast to dKO satellite cells, almost all WT, 1KO and 3KO satellite cells did not express these proliferative and myogenic markers. These results indicate that most of the dKO satellite cells were not in an undifferentiated quiescent state in adult skeletal muscle.

dKO satellite cells do not enter the undifferentiated quiescent state

The dKO satellite cells exhibited an impairment in their normally undifferentiated quiescent state in adult skeletal muscle. To determine whether this unusual state of dKO satellite cells results from a failure of entry into, or an impairment in the maintenance of, the undifferentiated quiescent state, we examined the frequency and number of undifferentiated quiescent satellite cells (Pax7$^+$ MyoD$^-$ Ki67$^-$ cells) from postnatal day 7 (P7) to P56. In P7 muscle, most Pax7$^+$ cells were not undifferentiated quiescent satellite cells, as described previously (Fig. 4A,B) (Pallafacchina et al., 2010), but the frequency and number of undifferentiated quiescent satellite cells increased in 4- to 8-week-old 3KO mice (Fig. 4B,C). However, such an increase in undifferentiated quiescent satellite cells was not observed in dKO mice. Examination of the frequency of Pax7$^+$ MyoD$^-$ and of Pax7$^+$ Ki67$^-$ cells showed similar results (Fig. 4D). These results indicate that dKO mice do not successfully generate undifferentiated quiescent satellite cells during postnatal development.

Hesr1 and Hesr3 are essential for the generation of reserve cells in vitro

To elucidate the characteristics of dKO satellite cells, satellite cells were isolated from 6- to 13-week-old 3KO and dKO mice. Even though the same numbers of cells were plated on culture dishes, a significant decrease in the number of dKO satellite cells was observed after being cultured in a growth medium (GM) for 3 days. To examine the proliferative potential of dKO satellite cells, an EdU-uptake assay was performed. As shown in Fig. 5A, the frequency of EdU$^+$ myoblasts was similar in dKO and 3KO cultures. To examine the survival of dKO satellite cells, freshly isolated satellite cells were cultured in GM for 24 hours and then a TUNEL assay was performed. As shown in Fig. 5B, a significantly increased number of TUNEL$^+$ cells was detected in dKO satellite cells.

We next investigated the survival of dKO satellite cells by clonal analysis. After isolating satellite cells from limb muscles of 6- to 13-week-old WT, 1KO, 3KO and dKO mice, satellite cells were cultured for 1 week. dKO satellite cell survival was lower than that of WT, 1KO and 3KO satellite cells (Fig. 5C). Low survival of dKO satellite cells was restricted to the period just after isolation from skeletal muscle, as dKO satellite cells that survived proliferated normally (Fig. 5D). These results suggest that Hesr1 and Hesr3 are not necessary for satellite cell proliferation in vitro.

To examine the roles of Hesr1 and Hesr3 in the generation of reserve cells (an in vitro model of in vivo undifferentiated quiescent satellite cells), 1×10^4 satellite cells derived from 3KO and dKO mice were cultured and allowed to differentiate in differentiation medium (DM) for 3.5 days. As shown in Fig. 5E, the fusion index of dKO satellite cells was slightly higher than that of 3KO satellite cells. By contrast, the frequency of reserve cells in dKO was substantially lower than that in WT, 1KO and 3KO satellite cell cultures (Fig. 5F). In dKO satellite cell cultures, the number of Pax7$^+$ cells was already reduced in DM by 1.5-2 days (Fig. 5G). Because almost all Pax7$^+$ cells expressed MyoD in both 3KO and dKO in GM (see Fig. S4 in the supplementary material), the loss of the Pax7$^+$ MyoD$^-$ population in dKO satellite cells was unlikely to affect this result. In addition, re-expression of Hesr3 was detected in Pax7$^+$ cells in DM (Fig. 5H), and an increase in the number of apoptotic cells was not observed in dKO satellite cells in DM (data not shown). Therefore, these results indicate that Hesr1 and Hesr3 are necessary for the generation of undifferentiated satellite cells.

Gradual decrease in the number of dKO satellite cells in adult skeletal muscle

Since dKO satellite cells were not maintained in an undifferentiated quiescent state, we investigated the change in satellite cell numbers with age. As shown in Fig. 6A, a significant decrease in the number of Pax7$^+$ satellite cells (80% of control) was observed in P7 dKO compared with 3KO mice. There is the possibility that the diminished satellite cell number at the neonatal stage leads to the

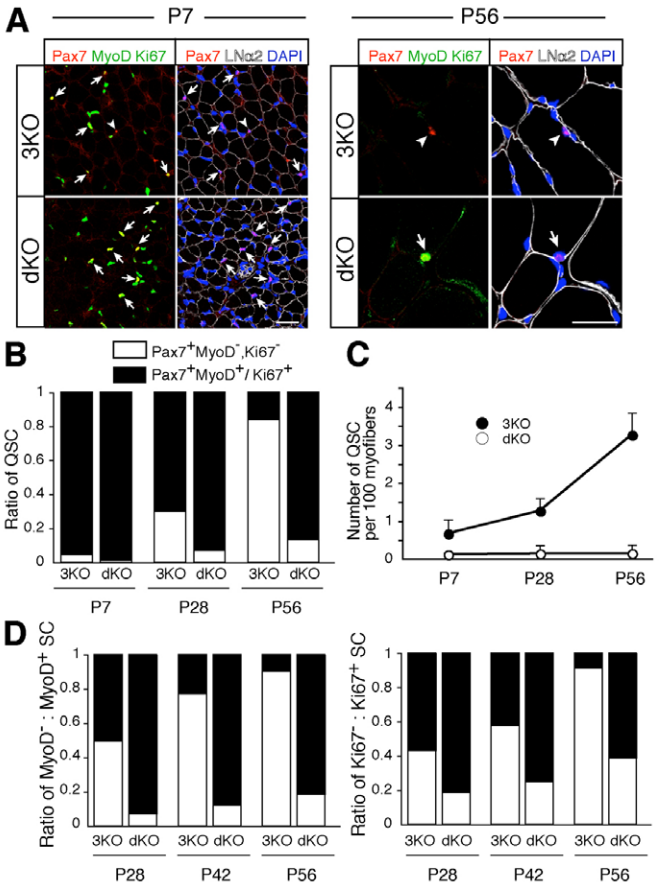

Fig. 4. Failure of dKO satellite cells to enter the undifferentiated quiescent state. (**A**) Quantitative analysis of undifferentiated quiescent satellite cells in uninjured TA muscle at P7 and P56. Arrows and arrowheads indicate differentiated non-quiescent (Pax7$^+$, Ki67$^+$/MyoD$^+$) and undifferentiated quiescent (Pax7$^+$, Ki67$^-$, MyoD$^-$) satellite cells, respectively. Pax7, red; MyoD/Ki67, green; laminin α2, white; DAPI, blue. Scale bars: 25 μm. (**B**) Ratio of undifferentiated quiescent (white) to differentiated non-quiescent (black) satellite cells in uninjured TA muscle of dKO and littermate 3KO mice at the indicated ages. The value shown is an average of the results of experiments conducted with three to four mice. (**C**) The number of undifferentiated quiescent satellite cells in B. The *y*-axis shows the mean number of satellite cells per 100 cross-sectional myofibers with s.d. (**D**) Relative ratio of MyoD$^-$ (white) to MyoD$^+$ satellite cells (black) and Ki67$^-$ (white) versus Ki67$^+$ satellite cells (black). The value shown is an average of the results of experiments conducted with three mice. The *x*-axis indicates the age of the mice analyzed.

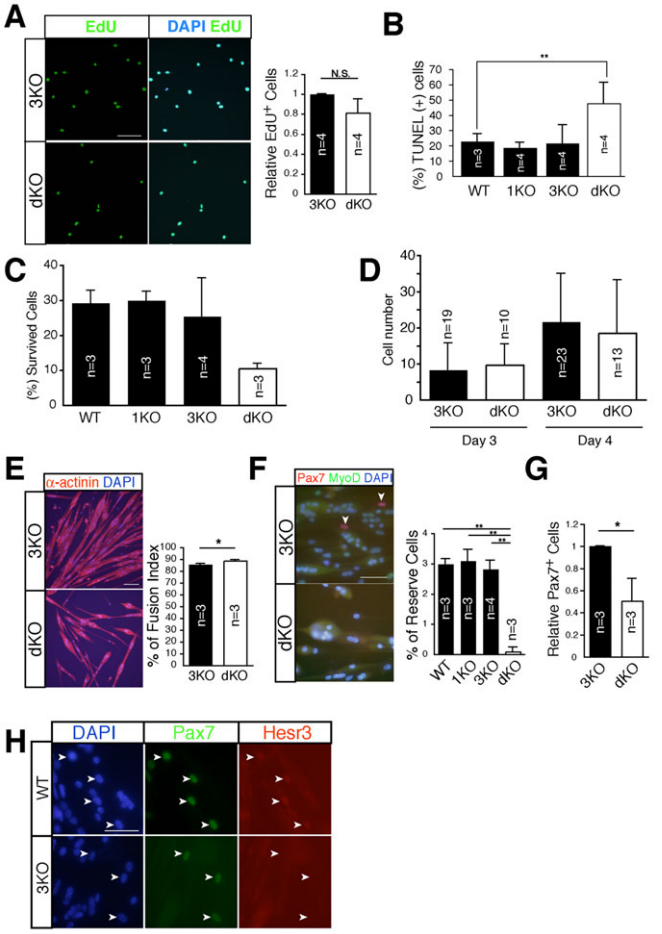

Fig. 5. Hesr1 and Hesr3 influence the generation of reserve cells. (**A**) EdU (green) uptake of primary myoblasts derived from dKO or littermate 3KO mice. Nuclei were stained with DAPI (blue). The *y*-axis shows the mean value with s.d. (*n*=4). (**B**) Freshly isolated satellite cells were cultured in GM for 24 hours and then TUNEL staining was performed. The *y*-axis shows the mean value of TUNEL$^+$ cells with s.d. (*n*=3-4). (**C**) Clonal analysis of satellite cells derived from WT, 1KO, 3KO and dKO mice, showing the frequency of colony-forming cells after 7 days in culture. (**D**) Cell number in colonies derived from single satellite cells cultured for 3 or 4 days. Colony number is shown in each bar. (**E**) Fusion index of primary myoblasts derived from dKO and littermate 3KO mice. Myotubes were stained with anti-sarcomeric α-actinin antibody (red) and DAPI (blue). The bar chart shows the mean percentage of the fusion index with s.d. (*n*=3). (**F**) Reserve cell frequencies of primary myoblasts derived from WT, 1KO, 3KO and dKO mice. The cells were stained with anti-Pax7 (red), anti-MyoD (green) and with DAPI (blue). Arrowheads indicate Pax7$^+$ MyoD$^-$ mononuclear reserve cells. The bar chart shows the mean percentage of reserve cells with s.d. (*n*=3-4). (**G**) Relative number of Pax7-expressing cells derived from 3KO and dKO mice in differentiation medium (DM) for 1.5-2 days. The y-axis shows the mean value with s.d. (*n*=3). Six- to 13-week-old mice were used in these experiments. (**H**) The cells were cultured in DM for 3 days and stained with anti-Pax7 (green), anti-Hesr3 (red) and DAPI (blue). Arrowheads indicate Pax7$^+$ mononuclear cells. *, P<0.05; **, P<0.01. Scale bars: 100 μm in E; 50 μm in A,F,H.

loss of muscle weight in dKO mice (Fig. 2A, see Fig. S2B in the supplementary material). Similar to previous reports (White et al., 2010), the number of satellite cells in littermate 3KO mice was constant after P28 (Fig. 6A). By contrast, the number of satellite cells in dKO mice decreased even after P28. To follow the decline of the satellite cell pool in dKO mice further, we stained satellite cells using anti-M-cadherin antibody. As shown in Fig. 6B, we obtained a result similar to that of the Pax7-staining experiment. In addition, the satellite cell frequency observed in the flow cytometry experiment indicated that the satellite cell number continued to gradually decrease even after the age of 6 weeks (Fig. 6C). These results suggest that the number of satellite cells in dKO mice was continuously decreasing even beyond the age of 4 weeks, by which time the satellite cell number has stabilized in 3KO mice.

There are two possible mechanisms for the diminution of satellite cell numbers in dKO muscle: cell death or accelerated cell fusion. We did not detect TUNEL$^+$ satellite cells in dKO muscle in vivo, although more than 4000 M-cadherin$^+$ cells were counted at P7, P28, P56 and P80 (data not shown). We next examined the

DEVELOPMENT

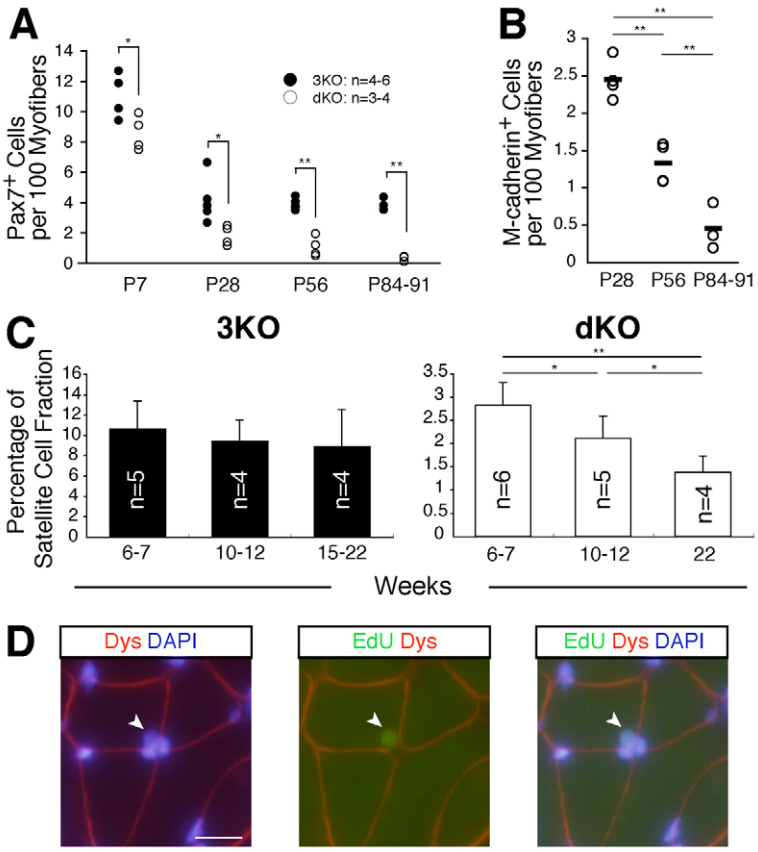

Fig. 6. The number of dKO satellite cells gradually decreases with age. (**A**,**B**) The *y*-axis indicates the number of Pax7$^+$ (A) or M-cadherin$^+$ (B) cells per 100 cross-sectional TA myofibers in dKO (white circles) and 3KO (black circles) mice. The *x*-axis indicates the age of the analyzed mice. (**C**) Quantitative analyses of satellite cell number by flow cytometry. The *y*-axis shows the percentage of SM/C-2.6$^+$ CD31$^-$ CD45$^-$ Sca1$^-$ (satellite) cells in dKO and 3KO 6- to 22-week-old mice. Error bars indicate s.d. The number of mice used in each study is shown. (**D**) Immunostaining of EdU (green) and dystrophin (Dys, red) and DAPI staining (blue) in dKO TA muscle. EdU$^+$ myofiber nuclei (arrowhead) were detected in dKO TA muscle. *, P<0.05; **, P<0.01. Scale bar: 20 μm.

possibility of accelerated cell fusion. Because many dKO satellite cells exhibited Ki67 expression in 6- to 8-week-old mice, 6- to 8-week-old dKO mice were injected with EdU three times, and, 2-3 weeks later, the muscles were fixed and observed. EdU$^+$ myonuclei, which located beneath the dystrophin, were detected in dKO myofibers (Fig. 6D). The average number of EdU$^+$ myonuclei per section was 0.13 and 0.33 in 3KO and dKO, respectively (n=3). Because, in general, DNA synthesis is not observed in myonuclei (Moss and Leblond, 1971), these results suggest that dKO satellite cells fused with the myofibers.

A remarkable regeneration defect in dKO mice with age

In dKO mice, immunohistological and flow cytometry studies showed satellite cell number decreases estimated to be 30-60%, 20-40% and less than 20% relative to satellite cell numbers in 4-, 8- and 20-week-old control mice, respectively (Fig. 7A). To investigate the relationship between the regenerative potential and the age of dKO mice, we injected cardiotoxin (CTX) into the TA muscle of 4-, 8- and 20-week-old mice (Fig. 7A). Three days after CTX injection, many M-cadherin$^+$ cells were observed in the regenerating TA muscle of both 4- and 8-week-old 3KO mice. However, the number of M-cadherin$^+$ cells was significantly lower in 8-week-old than in 4-week-old dKO mice (Fig. 7B). Furthermore, 4 days after CTX injection, 8-week-old dKO mice showed a greater decrease in the embryonic myosin heavy chain (eMyHC)$^+$ myotube area than 4-week-old mice (Fig. 7C). Similar to the finding for M-cadherin$^+$ cells, there was no significant difference in the eMyHC$^+$ area of 4- and 8-week-old 3KO mice. Similar to the situation for satellite cell numbers, the eMyHC$^+$ area of 4- and 8-week-old dKO mice was 30-60% and 10-30% of that of control mice, respectively. Consistent with the in vitro results, an in vivo EdU-uptake assay also indicated that the proliferative potentials of dKO and 3KO satellite cells were similar (Fig. 7D). These results suggested that the substantial decrease in M-cadherin$^+$ cells and eMyHC$^+$ area with age are the result of a diminished satellite cell pool in dKO mice.

We also examined the regenerative potential of dKO mice at a later stage, 14 days after injury. As shown in Fig. 7E, the injured muscle weight of dKO mice showed a tendency to decrease when mice were injected with CTX at 4 weeks of age. Consistent with the trend in satellite cell number, dKO mice injected with CTX at 8 and 20 weeks of age exhibited a remarkable loss of muscle weight (Fig. 7E). By contrast, WT, 1KO and 3KO mice did not show such a decrease in muscle weight after CTX injection.

The histological results also confirmed that there was a decrease in regeneration potential in dKO mice with age. In 3KO mice, normal regenerative potential was observed regardless of age (Fig. 7F,G). By contrast, 4-week-old dKO mice showed a slight loss of myofiber number without any fat or fibrosis accumulation (Fig. 7F,G, see Fig. S5 in the supplementary material). One of the 8-week-old dKO mice examined showed increased fat and fibrosis (3.57% and 19.7%, respectively), whereas the rest did not. In contrast to the 8-week-old dKO mice, 20-week-old mice showed significant fat and fibrosis accumulation, with a decrease in the number and area of myofibers compared with 4-week-old dKO and littermate control mice (Fig. 7F,G, see Fig. S5 in the supplementary material). These results indicate that the satellite cell number decreases with age and that this underlies the impaired skeletal muscle regeneration in dKO mice.

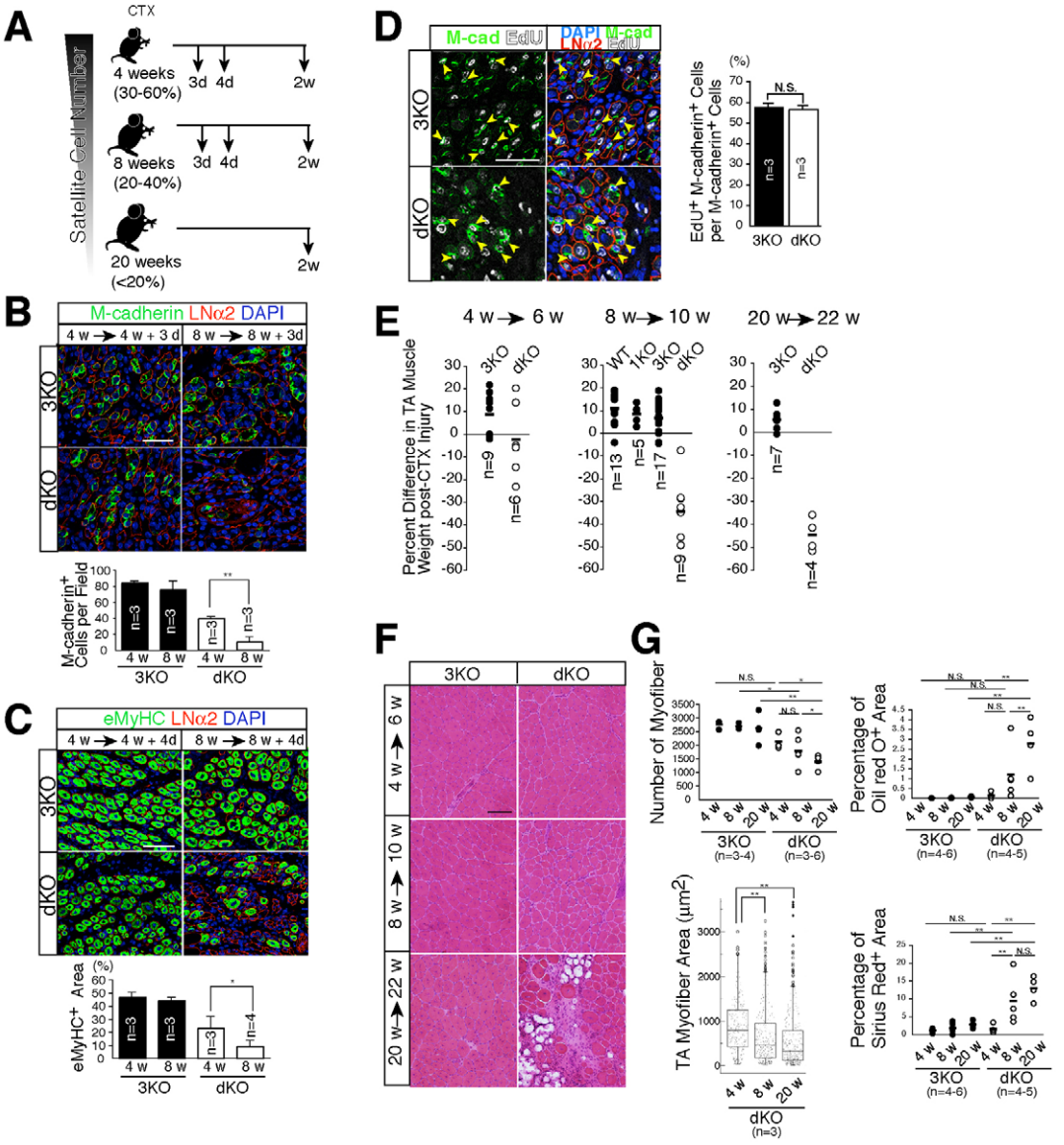

Fig. 7. Age-dependent regeneration defect in dKO mice. (**A**) Cardiotoxin (CTX) time scheme for analysis of the regenerative potential of each age group. The percentage value indicates the estimated frequency of dKO satellite cells compared with that of 3KO mice. (**B**) Immunostaining of M-cadherin (green) and laminin α2 (red) and DAPI staining (blue) in injured muscle 3 days after CTX injection. The *y*-axis shows the number of M-cadherin$^+$ cells per field in dKO or littermate 3KO mice. Error bars indicate the mean with s.d. (**C**) Immunostaining of embryonic myosin heavy chain (eMyHC, green) and laminin α2 (red) and DAPI staining (blue) in injured muscle 4 days after CTX injection. The *y*-axis shows the eMyHC$^+$ area (percentage) in dKO or littermate 3KO mice. Error bar indicates the mean with s.d. (**D**) In vivo EdU (white) uptake of M-cadherin$^+$ cells (green) in injured muscle 3 days after CTX injection of dKO or littermate 3KO mice. Red indicates laminin α2 expression. Nuclei were stained with DAPI (blue). Arrowheads indicate EdU$^+$ M-cadherin$^+$ cells. The *y*-axis shows the mean percentage of EdU$^+$ cells in M-cadherin$^+$ cells with s.d. (**E**) The change in TA muscle weight after regeneration. Each circle (WT, 1KO and 3KO, black; dKO, white) indicates the result of one mouse. Bar indicates the mean value of each group. (**F**) TA muscles of 3KO and dKO mice were examined histologically 2 weeks after CTX injection. Transverse sections were stained with H&E. (**G**) Quantitative analyses of the number and area of myofibers, the Oil Red O$^+$ area and the Sirius Red$^+$ area in injured muscles. Each circle (3KO, black; dKO, white) indicates the result of one mouse. Bar indicates the mean value of each group. *, P<0.05; **, P<0.01; N.S., non-significant difference. Scale bars: 25 μm in B; 50 μm in C,D,F.

DISCUSSION

Notch signaling regulates stem cells in many different tissues, including the nervous system, hematopoietic system, skin and intestine. Several studies indicate that it plays essential roles in skeletal muscle as well. Vasyutina et al. reported that deletion of *Rbpj* in the myogenic cells of *Pax3-Cre* or *Lbx1-Cre* transgenic mice leads to premature differentiation of the myogenic progenitor pool (Vasyutina et al., 2007). As a result, the complete loss of satellite cells in E18.5 distal limb muscle and severe skeletal muscle hypotrophy with a decreased number of myonuclei were observed in these mice. Schuster-Gossler et al. showed similar results using *Dll1* mutant mice (Schuster-Gossler et al., 2007).

Hes1, the major downstream target of Notch signaling, regulates the differentiation of multiple cell types (Kageyama et al., 2000). However, there is no apparent skeletal muscle phenotype in *Hes1*-null mice (Kageyama et al., 2000). In addition, *Hesr1* and *Hesr3*

are predominantly induced by stimulation of C2C12 cells with Dll4, which is one of the Notch ligands, whereas induction of *Hesr2* and Hes family genes was not observed (Buas et al., 2009). We also observed *Hesr1* and *Hesr3*, but not *Hesr2* and *Hes1*, expression in primary myoblasts stimulated with Dll1 (see Fig. S6A in the supplementary material).

In the present study, we showed *Hesr1* and *Hesr3* expression in neonatal and adult satellite cells and examined the physiological roles of Hesr1 and Hesr3 in skeletal muscle. Furthermore, upregulation of *Hes1* and *Hesr2* was not observed in dKO satellite cells (see Fig. S6B in the supplementary material). However, the phenotype of *Rbpj* mutant mice is different from that of the *Hesr1/3* dKO. In contrast to *Rbpj* mutant mice, *Hesr1/3* dKO mice show slight losses of the satellite cell pool and decreases in myofiber number at P7 (data not shown). Therefore, although Hesr1 and Hesr3 might play some role, they are not essential effector genes of Notch signaling in embryogenesis. Conboy et al. indicated that downregulation of Notch signaling leads to impaired regeneration in adult skeletal muscle (Conboy et al., 2003). In addition, they showed that Notch signaling was necessary for the proliferation of satellite cells. However, in this study, *Hesr1/3* dKO satellite cells exhibited normal proliferation in vitro and in vivo. These results suggest that Notch-mediated proliferation of satellite cells is not dependant on Hesr1 and Hesr3.

Each Hesr family gene is specifically expressed in particular tissues (Leimeister et al., 1999; Nakagawa et al., 1999). Their important roles in the heart and vascular system during development have been revealed using knockout mice. In contrast to *Hesr2* knockout mice, *Hesr1* and *Hesr3* knockout mice exhibit no obvious phenotype. However, a combined defect of *Hesr1* and *Hesr3* leads to ventricular septum defects with impairment of the mesenchymal-epithelial transition in the heart (Fischer et al., 2007). It has been reported that Hesr1 and Hesr2 functions overlap in cardiovascular development (Fischer et al., 2004; Kokubo et al., 2005b). Redundancy among Hes family members has also been reported (Fischer and Gessler, 2007). Thus, the effect of redundancy among Hesr or Hes family members is observed in multiple tissues and organs. In this report, we showed a new complementary effect of Hesr1 and Hesr3 in skeletal muscle physiology, especially in muscle satellite cells. In addition, during *Hesr1/3* dKO heart development, the incidence of ventricular septum defects was not 100% (but 21% in F2 and 82% in F9). However, all of our F7 dKO mice showed decreased satellite cell numbers, demonstrating the significance of Hesr1/3 in muscle satellite cells. Combinations of Hesr family and/or Hes family genes might also play central roles in the regulation of other stem cells to maintain diverse tissue homeostasis.

All tissue stem cells are maintained in an undifferentiated and quiescent state, and this state is considered to be essential for their long-term maintenance. Imayoshi et al. showed that adult neural stem cells differentiate into neurons via transit-amplifying cells that eventually result in complete neural stem cell depletion in *Rbpj* conditional knockout mice crossed with tamoxifen-inducible *Nestin-CreERT2* mice (Imayoshi et al., 2010). This indicates that the undifferentiated quiescent state is essential to sustain stem cell pools and that the lack of these mechanisms leads to loss of the stem cell compartment via premature differentiation. As shown here, most dKO satellite cells do not enter into the undifferentiated quiescent state during postnatal development. MyoD and myogenin are essential for myogenic differentiation. Therefore, the unusual MyoD and myogenin expression in dKO satellite cells leads to a loss of the satellite cell pool due to fusion with myofibers. Asakura et al. observed that MyoD expression is related to cell survival and that *Myod*-null myoblasts possess remarkable resistance to apoptosis compared with WT myoblasts in vitro (Asakura et al., 2007). In vitro, dKO satellite cells exhibit low survival in the period just after starting the culture. However, we observed no evidence for increased apoptosis in dKO mice in vivo and others have reported no evidence of $TUNEL^+$ cells in the premature myogenic progenitor cells of *Rbpj* or *Dll1* mutant mice during embryonic myogenesis (Schuster-Gossler et al., 2007; Vasyutina et al., 2007). These results suggest that, in vivo, dKO satellite cells undergo differentiation rather than cell death, although we cannot exclude the possibility that a low-level increase in programmed cell death contributes to the decrease in satellite cell number. Although dKO satellite cells exhibit premature differentiation but not cell death, we did not observe transient hypertrophy in dKO mice. This result suggests that: (1) a deficiency of Hesr1/3 does not accelerate cell cycle progression, but prolongs the entrance of satellite cells into quiescence; and/or (2) a slightly lower number of satellite cells in postnatal dKO mice obscured any transient hypertrophy.

Pax7-deficient mice exhibit severe loss of satellite cells and regeneration potential (Kuang et al., 2006; Seale et al., 2000). However, a recent study using mice with inducible and conditional Pax7 inactivation indicated that adult satellite cells do not require Pax7 for their function and maintenance, but that satellite cells do require Pax7 for 3 weeks after birth (Lepper et al., 2009). It is possible that Hesr1/3 are also necessary for postnatal development, but not for the maintenance of the satellite cell pool in adult skeletal muscle, similar to Pax7. Therefore, analyses of conditional and satellite cell-specific *Hesr1/3* mutant mice will be necessary to examine the roles of Hesr1/3 in established adult satellite cells.

In conclusion, Hesr1 and Hesr3 play crucial roles in skeletal muscle homeostasis by regulating the undifferentiated quiescent state of satellite cells. Investigations of Hesr1/3 will help to elucidate the molecular regulation of satellite cells in both physiological and pathological conditions.

Acknowledgements
We thank Katherine Ono for comments on the manuscript.

Funding
This work was supported by the Japan Society for the Promotion of Science (JSPS) KAKENHI [18800023 to S.F.]; The Ministry of Education, Culture, Sports, Science and Technology (MEXT) KAKENHI [20700358 to S.F., 16300132 to H.Y.]; Intramural Research Grant for Neurological and Psychiatric Disorders of the National Center of Neurology and Psychiatry (NCNP) [22-1 to S.F.]; and the Nakatomi Foundation (to S.F.).

Competing interests statement
The authors declare no competing financial interests.

Supplementary material
Supplementary material for this article is available at
http://dev.biologists.org/lookup/suppl/doi:10.1242/dev.067165/-/DC1

References

Asakura, A., Hirai, H., Kablar, B., Morita, S., Ishibashi, J., Piras, B. A., Christ, A. J., Verma, M., Vineretsky, K. A. and Rudnicki, M. A. (2007). Increased survival of muscle stem cells lacking the MyoD gene after transplantation into regenerating skeletal muscle. *Proc. Natl. Acad. Sci. USA* **104**, 16552-16557.

Beauchamp, J. R., Heslop, L., Yu, D. S., Tajbakhsh, S., Kelly, R. G., Wernig, A., Buckingham, M. E., Partridge, T. A. and Zammit, P. S. (2000). Expression of CD34 and Myf5 defines the majority of quiescent adult skeletal muscle satellite cells. *J. Cell Biol.* **151**, 1221-1234.

Buas, M. F., Kabak, S. and Kadesch, T. (2009). Inhibition of myogenesis by Notch: evidence for multiple pathways. *J. Cell. Physiol.* **218**, 84-93.

Charge, S. B. and Rudnicki, M. A. (2004). Cellular and molecular regulation of muscle regeneration. *Physiol. Rev.* **84**, 209-238.
Conboy, I. M., Conboy, M. J., Smythe, G. M. and Rando, T. A. (2003). Notch-mediated restoration of regenerative potential to aged muscle. *Science* **302**, 1575-1577.
Dyczynska, E., Sun, D., Yi, H., Sehara-Fujisawa, A., Blobel, C. P. and Zolkiewska, A. (2007). Proteolytic processing of delta-like 1 by ADAM proteases. *J. Biol. Chem.* **282**, 436-444.
Fischer, A. and Gessler, M. (2007). Delta-Notch-and then? Protein interactions and proposed modes of repression by Hes and Hey bHLH factors. *Nucleic Acids Res.* **35**, 4583-4596.
Fischer, A., Schumacher, N., Maier, M., Sendtner, M. and Gessler, M. (2004). The Notch target genes Hey1 and Hey2 are required for embryonic vascular development. *Genes Dev.* **18**, 901-911.
Fischer, A., Steidl, C., Wagner, T. U., Lang, E., Jakob, P. M., Friedl, P., Knobeloch, K. P. and Gessler, M. (2007). Combined loss of Hey1 and HeyL causes congenital heart defects because of impaired epithelial to mesenchymal transition. *Circ. Res.* **100**, 856-863.
Fukada, S., Higuchi, S., Segawa, M., Koda, K., Yamamoto, Y., Tsujikawa, K., Kohama, Y., Uezumi, A., Imamura, M., Miyagoe-Suzuki, Y. et al. (2004). Purification and cell-surface marker characterization of quiescent satellite cells from murine skeletal muscle by a novel monoclonal antibody. *Exp. Cell Res.* **296**, 245-255.
Fukada, S., Uezumi, A., Ikemoto, M., Masuda, S., Segawa, M., Tanimura, N., Yamamoto, H., Miyagoe-Suzuki, Y. and Takeda, S. (2007). Molecular signature of quiescent satellite cells in adult skeletal muscle. *Stem Cells* **25**, 2448-2459.
Hirsinger, E., Malapert, P., Dubrulle, J., Delfini, M. C., Duprez, D., Henrique, D., Ish-Horowicz, D. and Pourquie, O. (2001). Notch signalling acts in postmitotic avian myogenic cells to control MyoD activation. *Development* **128**, 107-116.
Imayoshi, I., Sakamoto, M., Yamaguchi, M., Mori, K. and Kageyama, R. (2010). Essential roles of Notch signaling in maintenance of neural stem cells in developing and adult brains. *J. Neurosci.* **30**, 3489-3498.
Joe, A. W., Yi, L., Natarajan, A., Le Grand, F., So, L., Wang, J., Rudnicki, M. A. and Rossi, F. M. (2010). Muscle injury activates resident fibro/adipogenic progenitors that facilitate myogenesis. *Nat. Cell Biol.* **12**, 153-163.
Kadi, F., Charifi, N., Denis, C., Lexell, J., Andersen, J. L., Schjerling, P., Olsen, S. and Kjaer, M. (2005). The behaviour of satellite cells in response to exercise: what have we learned from human studies? *Pflugers Arch.* **451**, 319-327.
Kageyama, R., Ohtsuka, T. and Tomita, K. (2000). The bHLH gene Hes1 regulates differentiation of multiple cell types. *Mol. Cells* **10**, 1-7.
Kokubo, H., Miyagawa-Tomita, S. and Johnson, R. L. (2005a). Hesr, a mediator of the Notch signaling, functions in heart and vessel development. *Trends Cardiovasc. Med.* **15**, 190-194.
Kokubo, H., Miyagawa-Tomita, S., Nakazawa, M., Saga, Y. and Johnson, R. L. (2005b). Mouse hesr1 and hesr2 genes are redundantly required to mediate Notch signaling in the developing cardiovascular system. *Dev. Biol.* **278**, 301-309.
Kuang, S., Charge, S. B., Seale, P., Huh, M. and Rudnicki, M. A. (2006). Distinct roles for Pax7 and Pax3 in adult regenerative myogenesis. *J. Cell Biol.* **172**, 103-113.
Kuang, S., Kuroda, K., Le Grand, F. and Rudnicki, M. A. (2007). Asymmetric self-renewal and commitment of satellite stem cells in muscle. *Cell* **129**, 999-1010.
Kuroda, K., Tani, S., Tamura, K., Minoguchi, S., Kurooka, H. and Honjo, T. (1999). Delta-induced Notch signaling mediated by RBP-J inhibits MyoD expression and myogenesis. *J. Biol. Chem.* **274**, 7238-7244.
Lai, E. C. (2004). Notch signaling: control of cell communication and cell fate. *Development* **131**, 965-973.
Leimeister, C., Externbrink, A., Klamt, B. and Gessler, M. (1999). Hey genes: a novel subfamily of hairy- and Enhancer of split related genes specifically expressed during mouse embryogenesis. *Mech. Dev.* **85**, 173-177.
Lepper, C., Conway, S. J. and Fan, C. M. (2009). Adult satellite cells and embryonic muscle progenitors have distinct genetic requirements. *Nature* **460**, 627-631.
Mauro, A. (1961). Satellite cell of skeletal muscle fibers. *J. Biophys. Biochem. Cytol.* **9**, 493-495.
Megeney, L. A., Kablar, B., Garrett, K., Anderson, J. E. and Rudnicki, M. A. (1996). MyoD is required for myogenic stem cell function in adult skeletal muscle. *Genes Dev.* **10**, 1173-1183.
Moss, F. P. and Leblond, C. P. (1971). Satellite cells as the source of nuclei in muscles of growing rats. *Anat. Rec.* **170**, 421-435.
Nakagawa, O., Nakagawa, M., Richardson, J. A., Olson, E. N. and Srivastava, D. (1999). HRT1, HRT2, and HRT3: a new subclass of bHLH transcription factors marking specific cardiac, somitic, and pharyngeal arch segments. *Dev. Biol.* **216**, 72-84.
Pallafacchina, G., Francois, S., Regnault, B., Czarny, B., Dive, V., Cumano, A., Montarras, D. and Buckingham, M. (2010). An adult tissue-specific stem cell in its niche: a gene profiling analysis of in vivo quiescent and activated muscle satellite cells. *Stem Cell Res.* **4**, 77-91.
Sabourin, L. A. and Rudnicki, M. A. (2000). The molecular regulation of myogenesis. *Clin. Genet.* **57**, 16-25.
Schultz, E., Gibson, M. C. and Champion, T. (1978). Satellite cells are mitotically quiescent in mature mouse muscle: an EM and radioautographic study. *J. Exp. Zool.* **206**, 451-456.
Schuster-Gossler, K., Cordes, R. and Gossler, A. (2007). Premature myogenic differentiation and depletion of progenitor cells cause severe muscle hypotrophy in Delta1 mutants. *Proc. Natl. Acad. Sci. USA* **104**, 537-542.
Seale, P., Sabourin, L. A., Girgis-Gabardo, A., Mansouri, A., Gruss, P. and Rudnicki, M. A. (2000). Pax7 is required for the specification of myogenic satellite cells. *Cell* **102**, 777-786.
Segawa, M., Fukada, S., Yamamoto, Y., Yahagi, H., Kanematsu, M., Sato, M., Ito, T., Uezumi, A., Hayashi, S., Miyagoe-Suzuki, Y. et al. (2008). Suppression of macrophage functions impairs skeletal muscle regeneration with severe fibrosis. *Exp. Cell Res.* **314**, 3232-3244.
Uezumi, A., Ojima, K., Fukada, S., Ikemoto, M., Masuda, S., Miyagoe-Suzuki, Y. and Takeda, S. (2006). Functional heterogeneity of side population cells in skeletal muscle. *Biochem. Biophys. Res. Commun.* **341**, 864-873.
Uezumi, A., Fukada, S., Yamamoto, N., Takeda, S. and Tsuchida, K. (2010). Mesenchymal progenitors distinct from satellite cells contribute to ectopic fat cell formation in skeletal muscle. *Nat. Cell Biol.* **12**, 143-152.
Vasyutina, E., Lenhard, D. C., Wende, H., Erdmann, B., Epstein, J. A. and Birchmeier, C. (2007). RBP-J (Rbpsuh) is essential to maintain muscle progenitor cells and to generate satellite cells. *Proc. Natl. Acad. Sci. USA* **104**, 4443-4448.
White, R. B., Bierinx, A. S., Gnocchi, V. F. and Zammit, P. S. (2010). Dynamics of muscle fibre growth during postnatal mouse development. *BMC Dev. Biol.* **10**, 21.
Zammit, P. S., Golding, J. P., Nagata, Y., Hudon, V., Partridge, T. A. and Beauchamp, J. R. (2004). Muscle satellite cells adopt divergent fates: a mechanism for self-renewal? *J. Cell Biol.* **166**, 347-357.
Zhang, K., Sha, J. and Harter, M. L. (2010). Activation of Cdc6 by MyoD is associated with the expansion of quiescent myogenic satellite cells. *J. Cell Biol.* **188**, 39-48.

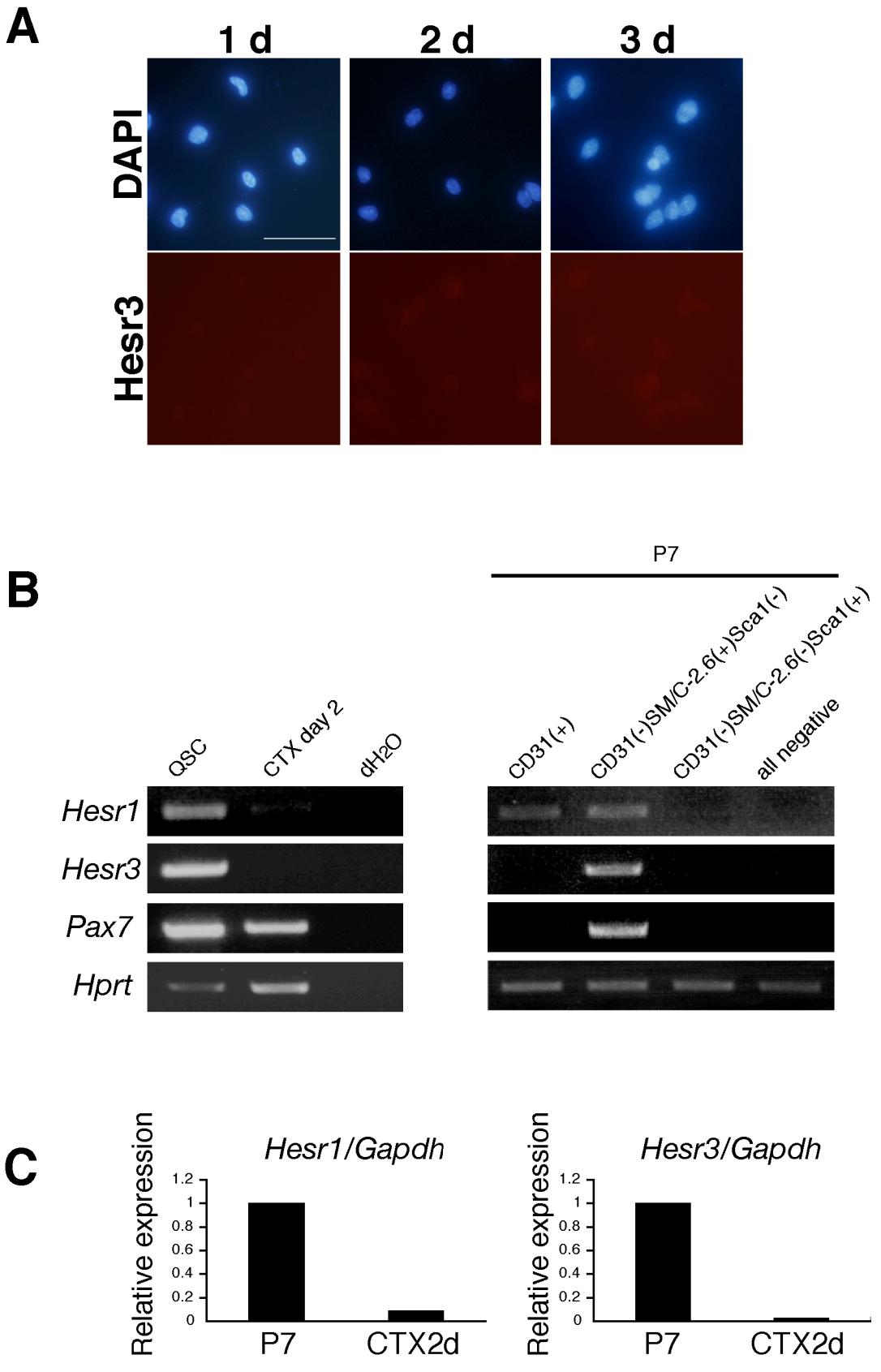
A
1 d
2 d
3 d
DAPI
Hesr3
B
P7
QSC
CTX day 2
dH2O
CD31(+)
CD31(-)SM/C-2.6(+)Sca1(-)
CD31(-)SM/C-2.6(-)Sca1(+)
all negative
Hesr1
Hesr3
Pax7
Hprt
C
Hesr1/Gapdh
Hesr3/Gapdh
Relative expression
1.2
1
0.8
0.6
0.4
0.2
0
P7
CTX2d

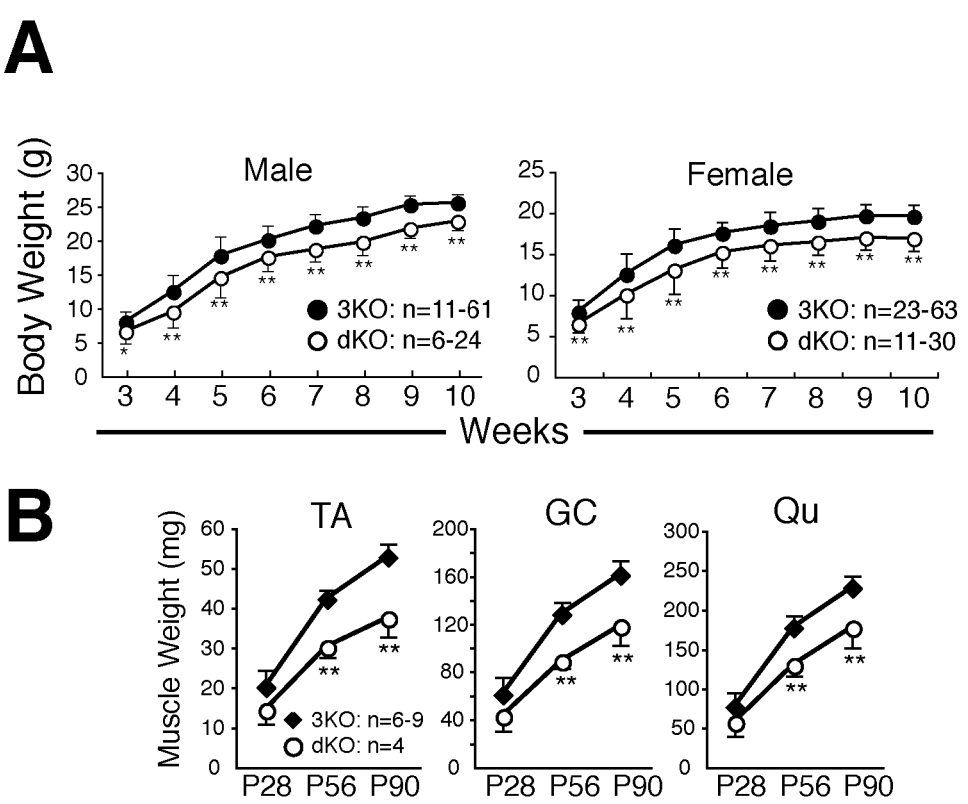
A
Body Weight (g)
Male
Female
3KO: n=11-61
dKO: n=6-24
3KO: n=23-63
dKO: n=11-30
Weeks
B
Muscle Weight (mg)
TA
GC
Qu
3KO: n=6-9
dKO: n=4
P28 P56 P90

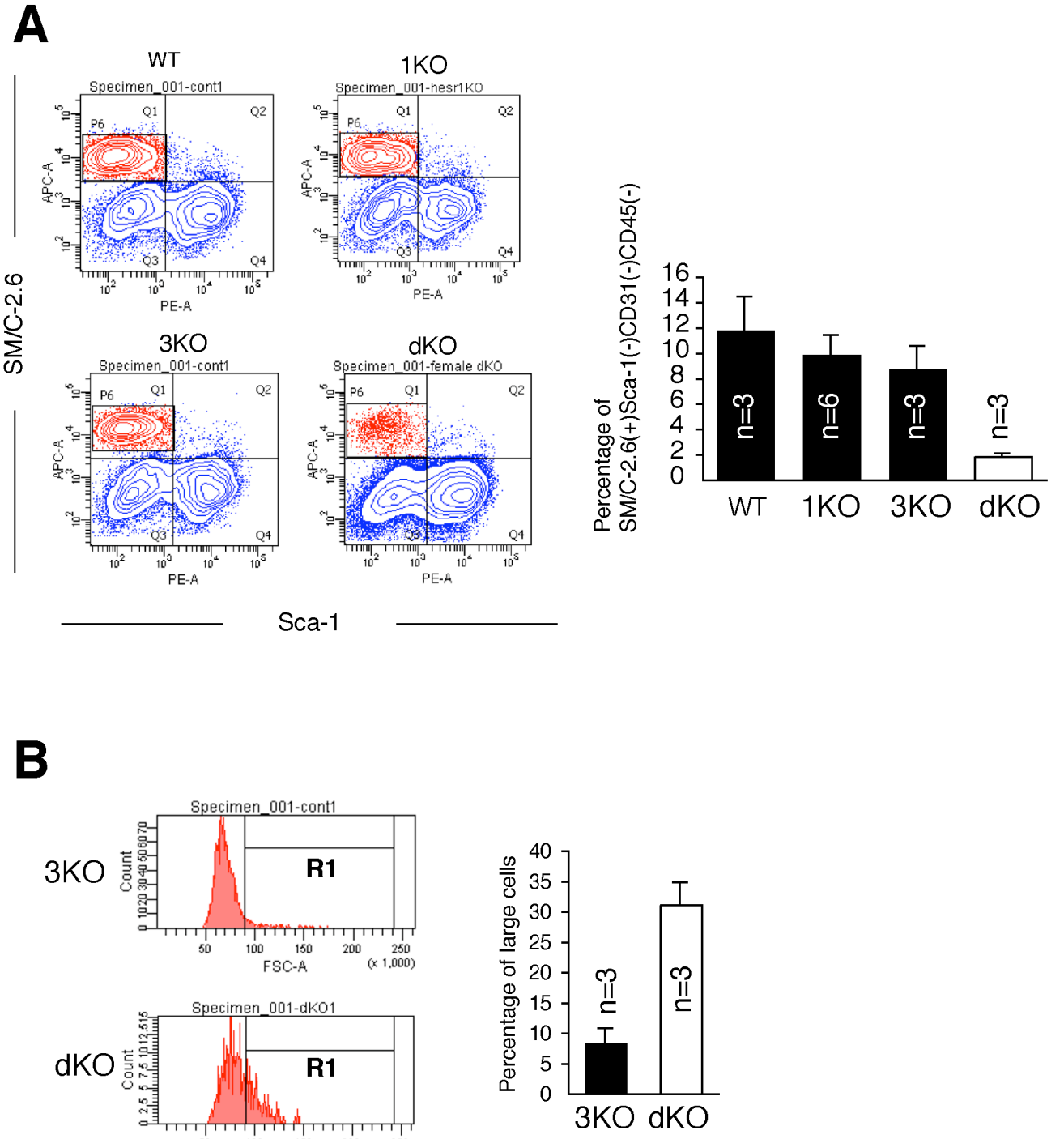
A
WT
1KO
3KO
dKO
Specimen_001-cont1
Specimen_001-hesr1KO
Specimen_001-female dKO
P6
Q1
Q2
Q3
Q4
APC-A
PE-A
SM/C-2.6
Sca-1
Percentage of SM/C-2.6(+)Sca-1(-)CD31(-)CD45(-)
n=3
n=6
n=3
n=3
WT
1KO
3KO
dKO
B
3KO
dKO
Specimen_001-cont1
Specimen_001-dKO1
R1
Count
FSC-A
(x 1,000)
Percentage of large cells
n=3
n=3
3KO
dKO

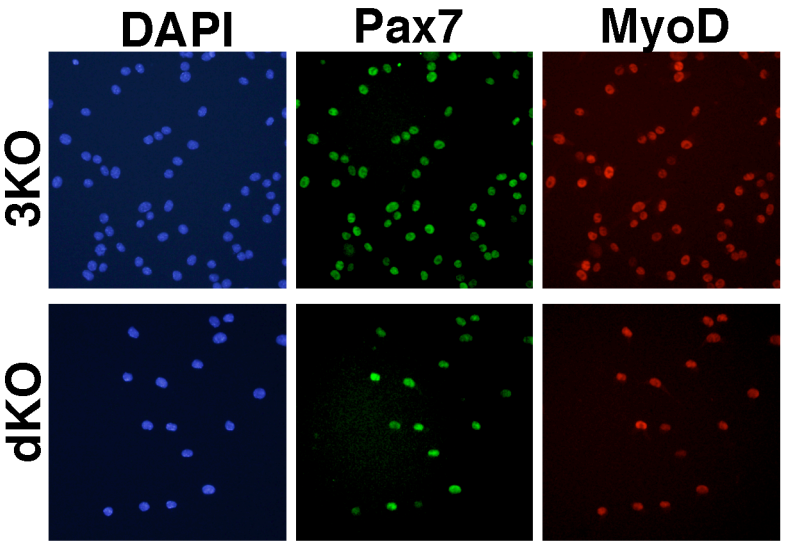
DAPI
Pax7
MyoD
3KO
dKO

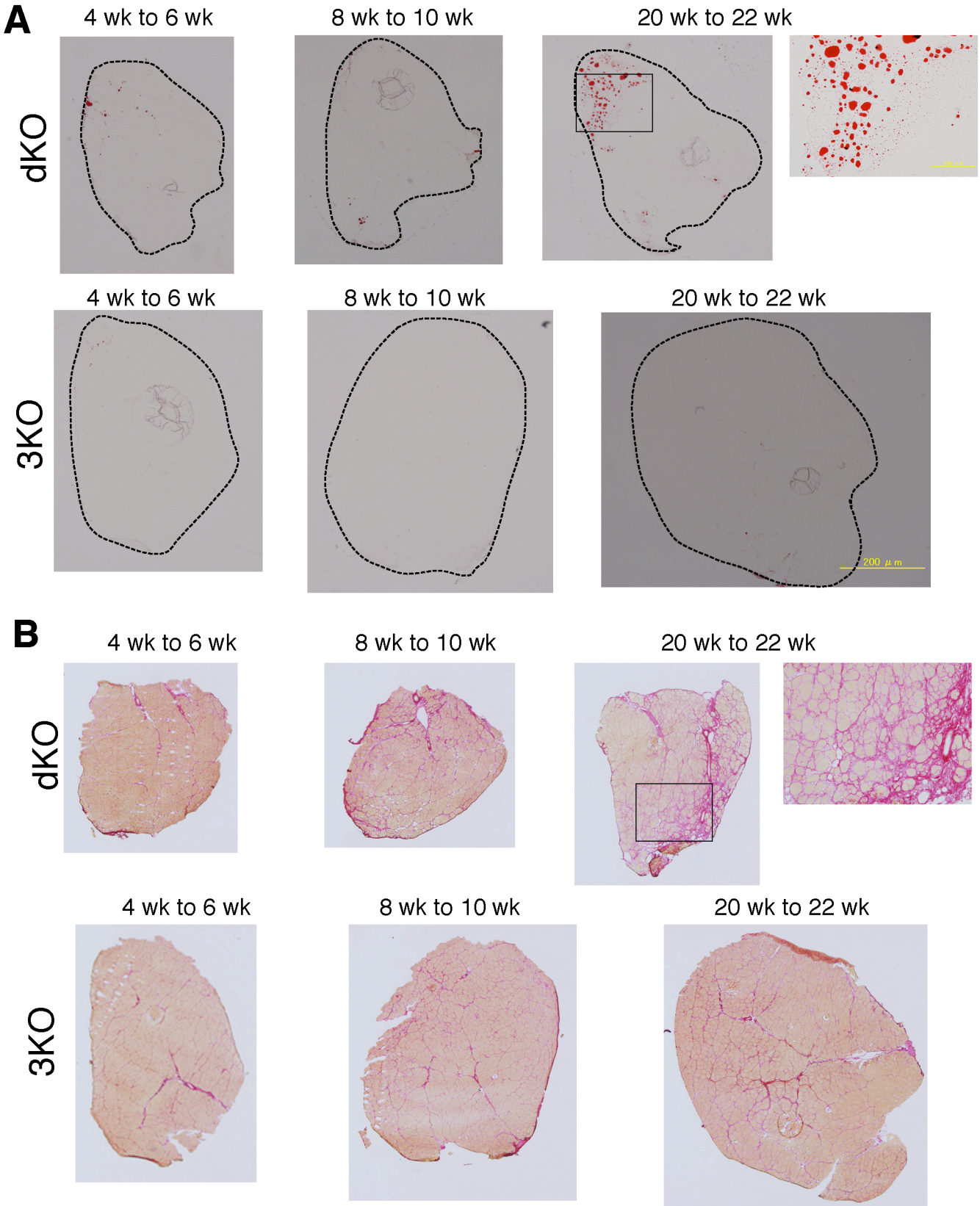
A
4 wk to 6 wk
8 wk to 10 wk
20 wk to 22 wk
dKO
4 wk to 6 wk
8 wk to 10 wk
20 wk to 22 wk
3KO
200 μm
B
4 wk to 6 wk
8 wk to 10 wk
20 wk to 22 wk
dKO
4 wk to 6 wk
8 wk to 10 wk
20 wk to 22 wk
3KO

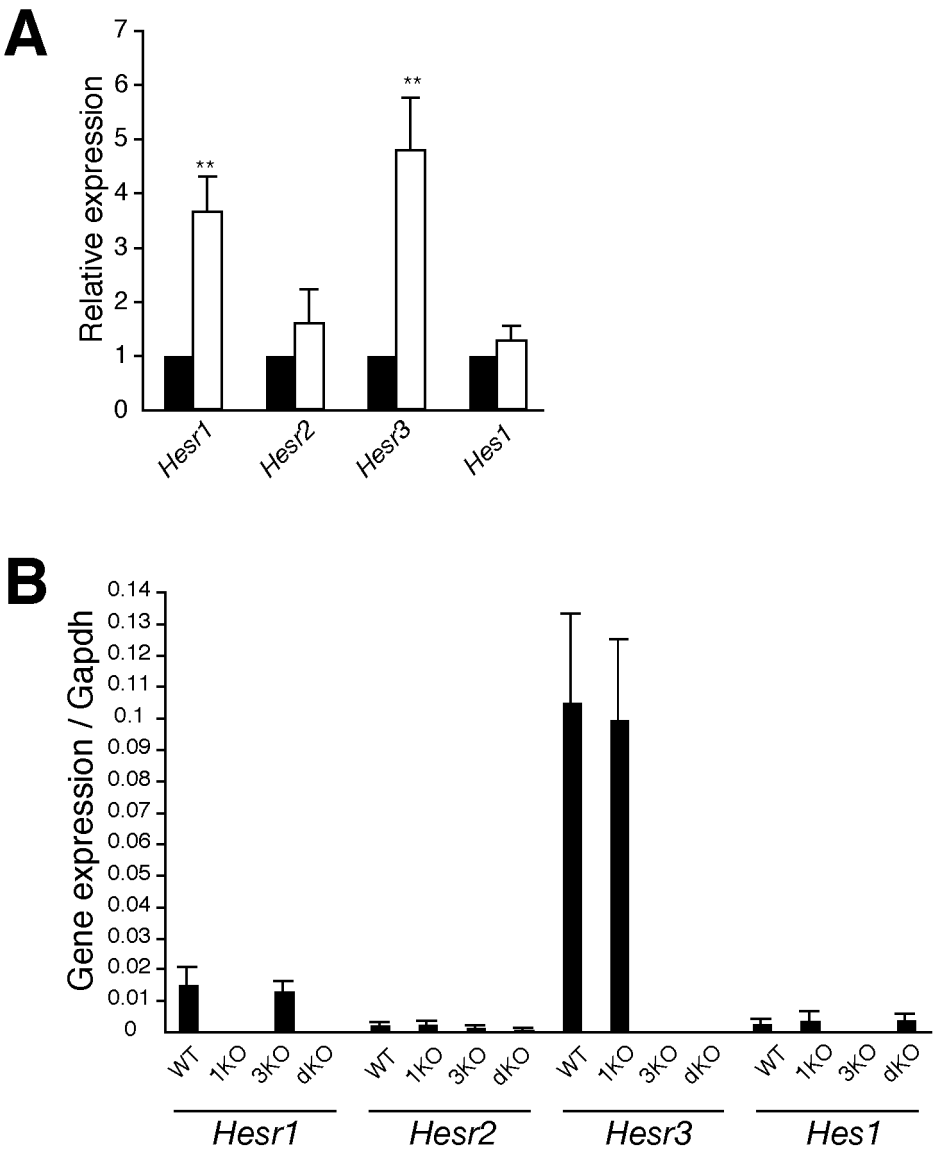
A
Relative expression
0
1
2
3
4
5
6
7
**
**
Hesr1
Hesr2
Hesr3
Hes1
B
Gene expression / Gapdh
0
0.01
0.02
0.03
0.04
0.05
0.06
0.07
0.08
0.09
0.1
0.11
0.12
0.13
0.14
WT
1KO
3KO
dKO
Hesr1
Hesr2
Hesr3
Hes1

Table S1. Primer sequences

Gene	Primer	Sequence (5′ to 3′)	Product size (bp)
Hprt	Fwd	CTTTGCTGACCTGCTGGATTACAT	361
	Rev	GTCAAGGGCATATCCAACAACAAA	
Gapdh	Fwd	CCTGGAGAAACCTGCCAAGTATG	133
	Rev	AGAGTGGGAGTTGCTGTTGAAGTC	
Hesr1	Fwd	CGACGAGACCGAATCAATAACAG	203
	Rev	CGAAACCCCAAACTCCGATAG	
Hesr2	Fwd	GTAACTGATGTCGTCCATTTCGG	424
	Rev	GCCTGCTTCTTCTCTTTCTCAACC	
Hesr3	Fwd	GTCCCCACTGCCTTTGAGA	342
	Rev	ACAGCTATGCAGGAAGGACCAGG	
Pax7	Fwd	GAAAGCCAAACACAGCATCGA	466
	Rev	ACCCTGATGCATGGTTGATGG	
Myf5	Fwd	TGCCATCCGCTACATTGAGAG	353
	Rev	CCGGGGTAGCAGGCTGTGAGTTG	
Pdgfra	Fwd	GACGAGTGTCCTTCGCCAAAGTG	341
	Rev	CAAAATCCGACCAAGCACGAGG	
Real-time PCR			
Gapdh	Fwd	TGTCAAGCTCATTTCCTGG	138
	Rev	TTGGGGGCCGAGTTGGGATA	
Gapdh (standard)	Fwd	GAAGGTGGTGAAGCAGGCATCT	366
	Rev	GTATTCAAGAGAGTAGGGAGGG	
Hesr1	Fwd	CGGACGAGAATGGAAACTTGA	50
	Rev	CCAAAACCTGGGACGATGTC	
Hesr1 (standard)	Fwd	AGATAGTGAGCTGGACGAGACC	331
	Rev	CCGAAACCCCAAACTCCGATAG	
Hesr2	Fwd	AAGCGCCCTTGTGAGGAAA	49
	Rev	TCGCTCCCCACGTCGAT	
Hesr2 (standard)	Fwd	AAGCGCCCTTGTGAGGAAA	371
	Rev	GTCAAGCACTCTCGGAATC	
Hesr3	Fwd	CAGCCCTTCGCAGATGCAA	100
	Rev	CCAATCGTCGCAATTCAGAAAG	
Hesr3 (standard)	Fwd	TCGATGTGGGTCAAGAGAACG	316
	Rev	TCCCGAAACCCAATACTCC	
Hes1	Fwd	TGAAGGATTCCAAAAATAAAATTCTCTGGG	363
	Rev	CTTGGAATGCCGGGAGCTATC	
Hes1 (standard)	Fwd	CTGTCTACCTCTCTCCTTGG	409
	Rev	CTTGGAATGCCGGGAGCTATC	